

Invited Paper

Quantitative AES at Interfaces

Pavel Lejček^{1*} and Siegfried Hofmann²¹Institute of Physics, AS CR, Na Slovance 2, 182 21 Praha 8, Czech Republic²Max-Planck-Institute for Metals Research, Heisenbergstr. 3, 70569 Stuttgart, Germany

*lejcekp@fzu.cz

(Received : October 3, 2010; Accepted : January 11, 2011)

Chemical composition of internal interfaces and especially grain boundaries differs from that of the grain interior and controls materials behavior. Application of the mostly spread method of surface analysis – Auger electron spectroscopy (AES) – for measurement of nanochemistry at these buried surfaces is complicated by necessity to open the boundary by intergranular brittle fracture. Consequently, the quantification of AES spectra must also take into account redistribution of the species, segregated at the boundary, between the two fracture surfaces. In this contribution, we analyze the transformation of AES spectra onto grain boundary concentrations using the standardless methods, which are reliable for determination of thermodynamic parameters characterizing the grain boundary segregation.

1. Introduction

Metallic materials used in technical practice are polycrystalline: They consist of both the huge number of small crystals (grains), which differ in mutual crystallographic orientations, and the grain boundaries separating them. The grain boundaries are internal surfaces characterized by an extra energy and thus, by altered interfacial properties. They often represent weak link of the structure and therefore, limit the materials application. In particular, there occurs grain boundary enrichment by solutes and impurities that is responsible for an embrittlement [1]. To describe generally the equilibrium enrichment – interfacial segregation – the Langmuir–McLean segregation isotherm is applied to provide us with the values of the thermodynamic parameters of the grain boundary segregation, the Gibbs energy, ΔG_I , [2]

$$\frac{X_I^\phi}{1 - X_I^\phi} = \frac{X_I}{1 - X_I} \exp\left(-\frac{\Delta G_I}{RT}\right) \quad (1)$$

relating the grain boundary concentration, X_I^ϕ , to the bulk concentration, X_I . ΔG_I in Eq. (1) is composed of enthalpy, ΔH_I , and entropy, ΔS_I ,

$$\Delta G_I = \Delta H_I - T\Delta S_I. \quad (2)$$

The values of the thermodynamic parameters

of interfacial segregation are very important for generalization of segregation data and their further application for predictive purposes [3]. The crucial condition to obtain reliable values of the segregation enthalpy and entropy is careful measurement and quantification of the grain boundary composition, X_I^ϕ , corresponding to chosen temperatures. In this way, the sample (a bicrystal with crystallographically characterized grain boundary at best) is long-term annealed at constant temperature, T_a , and quenched to room temperature to preserve the equilibrium state at T_a . To measure the grain boundary composition, a technique of surface analysis, usually Auger electron spectroscopy (AES), has frequently been used when applied on fracture surface of an in-situ intergranularly broken sample in ultra-high-vacuum ($<10^{-7}$ Pa). The brittle fracture is often facilitated by cooling the sample to a low temperature (e.g. by liquid nitrogen). The transformation of the AES spectra to grain boundary concentrations requires accounting for several assumptions.

The aim of this contribution is to discuss the specifics and quantification of AES spectra for application to grain boundary segregation.

2. Chemistry at Fracture Surfaces

As mentioned above, application of methods of surface analysis on chemistry of grain boundaries requires opening these interfaces by brittle

intergranular fracture. During this process, the segregated species are distributed between two newly created surfaces. Since usually one part of the fractured sample is only preserved for measurement, it is assumed that the segregands are equally (0.5:0.5) distributed between them. However, detail experiments showed that the distribution may be heterogeneous.

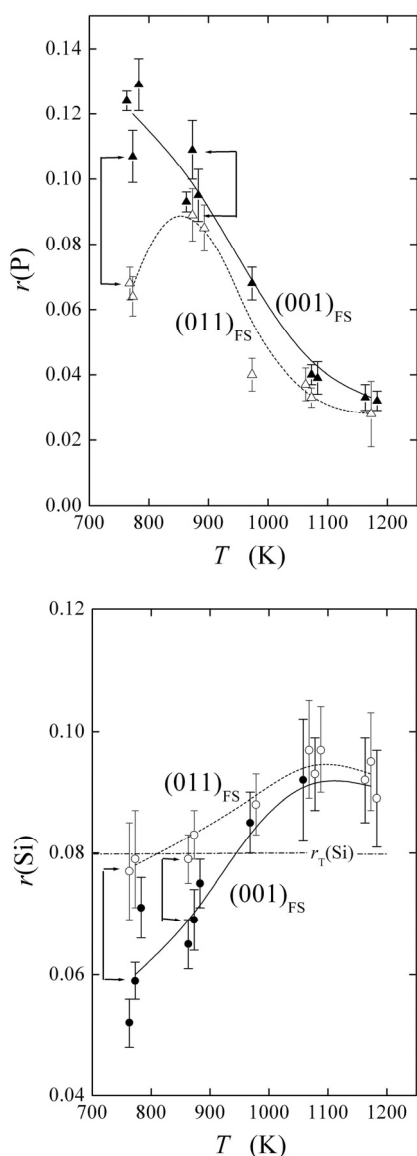


Fig. 1 Measured relative Auger intensities, $r(I)$, at both matching fracture surfaces (FS) of the $45^\circ[100]_1(001)/(011)_2$ asymmetrical tilt grain boundary in an Fe-4at%Si alloy, for phosphorus (above) and silicon (bottom) [4]. The intensity ratios are $r(I) = I_I/I_{Fe}$ for $(001)_{FS}$ (solid symbols, full lines) and $(011)_{FS}$ (empty symbols, dashed lines). The arrows connecting two points designate the one-to-one analysis at the same localities of the matching fracture surfaces. $r_t(Si)$ designates the value of $r(Si)$ corresponding to the bulk (transgranular) state.

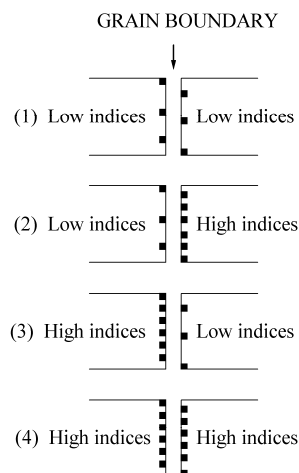


Fig. 2 Schematic depiction of solute segregation at the grain boundaries combined of the planes with low and high index (dark marks depict amount of segregand) (According to [5]).

The heterogeneity can originate from two sources, (i) different segregation to individual boundary planes due to their structure; and (ii) asymmetry of the fracture process.

The example of the former case is the measurement of the composition of the fracture surfaces of the $45^\circ[100]_1(001)/(011)_2$ asymmetrical tilt grain boundary in an Fe-4at%Si alloy (Fig. 1) [4]. The results exhibited systematic differences between the compositions of the two fracture surfaces: the fracture surface of the (011) boundary side with a denser structure exhibits a lower AES signal of phosphorus and a higher one of silicon than the (001) fracture surface. This was also proved by different intensities of Auger signals obtained from the matching points at both fracture surfaces [4]. The differences in the segregation to two matching planes of asymmetrical grain boundaries were first suggested by Suzuki *et al.* (Fig. 2) [5].

A heterogeneous distribution of segregands has also been detected at symmetrical grain boundaries, i.e. at interfaces formed by the matching planes of the same crystallography. Its origin is the asymmetry of the fracture process. It is known that segregation of embrittling metalloids (I) in metals (M) results in the formation of " M_xI clusters" with strong covalent-like bonds. Their formation weakens neighbor $M-M$ metallic bonds which are consequently broken during fracturing [6]. Therefore, the fracture does not pass directly through the boundary core but runs along a vicinal parallel plane. Since there are two identical paths of weakened bonds at both sides of the boundary core, the fracture can zig-zag between these two paths. This was proved for segregation of

phosphorus at the $36.9^\circ[100]$, $\{013\}$ symmetrical tilt grain boundary in an Fe-4at%Si alloy (Fig. 3) [7]. It is clearly seen in Fig. 3 that the total composition of the grain boundary does not change (taking into account the statistical scatter of the data) but sometimes, the fracture jumps from one path to another one. It means that at one locality, the fracture runs in front of the boundary core relatively to the detector and therefore, the AES signal is “enriched” by contributions of the subsurface layers, i.e. the phosphorus-rich grain boundary core. The signal taken from the localities behind the boundary where no phosphorus is present in deeper subsurface layers then indicates its lower concentrations. Based on these differences as well as on theoretical modeling it was shown that the core of the $\{013\}$ grain boundary consists of five layers (boundary core + two layers on both sides of the boundary), which are enriched by phosphorus, and that the path of the weakened metallic bonds is between the core plane and its neighbor on either side [7].

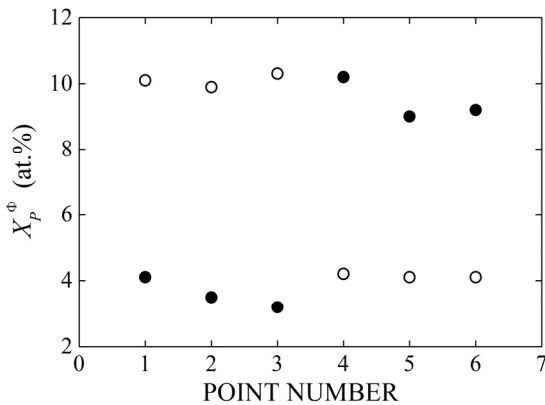


Fig. 3 Phosphorus concentration at several points in the high- and low-phosphorus regions on the matching fracture surfaces FS₁ (solid points) and FS₂ (empty points) of a broken bicrystal [7].

3. Quantification of AES Data of the Fracture Surfaces and Their Transformation to Grain Boundary Composition

A procedure used for quantification of the AES data and their transformation to the composition of complete grain boundary has to take into account the above facts on distribution of species between the two fracture surfaces as well as the possibility that this distribution does not need to be equal (i.e. one-to-one).

Let us suppose that the segregated layer at the grain boundary is monatomic of thickness δ and that the fracture opening the boundary for AES

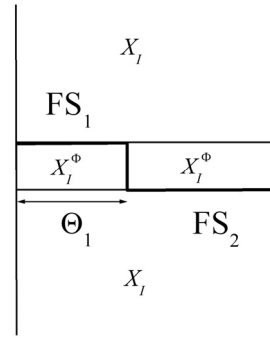


Fig. 4 Schematic representation of the fracture path opening the grain boundary by intergranular brittle fracture in a binary system $M-I$ of grain boundary and bulk compositions, X_I^ϕ and X_I , and monatomic segregation layer of thickness δ . FS₁ and FS₂ denote the fracture surfaces after fracture, and the thick drawn line marks the fracture path, Θ_1 is the total area of FS₁ [3,8].

measurements runs in a way schematically depicted in Fig. 4. The total area of remained segregated boundary is Θ_1 (Fig. 4) despite zig-zaging the boundary from one path to another one [8,9]. The total intensity of the AES signal coming from the whole fracture surface is

$$I_I = (I_I)_{FS_1} + (I_I)_{FS_2}$$

$$= I_I^0 \left\{ \begin{array}{l} X_I^\phi \left[1 - \exp\left(-\frac{\delta}{\lambda_{I,I}^0 \cos \theta}\right) \right] + \\ X_I \left[1 + \exp\left(-\frac{\delta}{\lambda_{I,I}^0 \cos \theta}\right) \right] \end{array} \right\}, \quad (3)$$

where

$$\left(\frac{I_I}{I_I^0} \right)_{FS_1} = \Theta_1 X_I^\phi \left[1 - \exp\left(-\frac{\delta}{\lambda_{I,I}^0 \cos \theta}\right) \right]$$

$$+ \Theta_1 X_I \exp\left(-\frac{\delta}{\lambda_{I,I}^0 \cos \theta}\right)$$

$$+ (1 - \Theta_1) X_I,$$

and

$$\left(\frac{I_I}{I_I^0} \right)_{FS_2} = (1 - \Theta_1) X_I \exp\left(-\frac{\delta}{\lambda_{I,I}^0 \cos \theta}\right) +$$

$$(1 - \Theta_1) X_I^\phi \left[1 - \exp\left(-\frac{\delta}{\lambda_{I,I}^0 \cos \theta}\right) \right]$$

$$+ \Theta_1 X_I.$$

In Eqs. (3)–(5), $\lambda_{I,I}^0$ is the effective attenuation length of Auger electrons of solute I in matrix I [10], θ is the emission angle relative to the surface normal and I_I^0 is the intensity of 100% bulk solute element [11]. Correspondingly,

$$X_I^\Phi = \frac{(I_I/I_I^0)_{FS_1} + (I_I/I_I^0)_{FS_2}}{1 - \exp[-\delta/(\lambda_{I,I}^0 \cos \theta)]} - X_I \frac{1 + \exp[-\delta/(\lambda_{I,I}^0 \cos \theta)]}{1 - \exp[-\delta/(\lambda_{I,I}^0 \cos \theta)]}. \quad (6)$$

I_I^0 is the “internal standard” obtained e.g. from measurements at the transgranular fracture [8]. The ratio technique proves the possibility of using relative sensitivity factors from handbooks (e.g. [12]). When the distribution of the solutes between two fracture surfaces is homogeneous (i.e. $(I_I)_{FS_1} = (I_I)_{FS_2}$ at symmetrical boundaries), we may simply double the measured signal of one fracture surface. In general $(I_I)_{FS_1} \neq (I_I)_{FS_2}$ and both fracture surfaces have to be studied [4].

The measurements of the absolute intensity are difficult and therefore, the signal intensities of elements are compared relatively each to the other and also relatively to the matrix. In this case, the backscattering factors $r_{I,I}$ (I in pure I) and $r_{I,M}$ (I in pure M) are taken into account.

If a solute enrichment also occurs in deeper atomic layers, the intensity of each layer, (i.e. the first term in Eq. (3), $1 - \exp[-d/(\lambda_{I,I}^0 \cos \theta)]$), has to be multiplied by the attenuation factor

$$f_w = \exp\left[-\frac{(\xi-1)\delta}{\lambda_{I,I}^0}\right] \quad (7)$$

accounting for inelastic and elastic scattering of Auger electrons. ξ denotes the number of the layer from the surface and the total intensity I_I of Auger electrons is given by a sum of the intensities from each atomic layer ξ [11],

$$\frac{I_I}{I_{I,w}^0} = \sum_{\xi=1}^N \xi X_I^\Phi \left\{ \exp\left[-\frac{(\xi-1)\delta}{\lambda_{I,I}^0}\right] - \exp\left[-\frac{\xi\delta}{\lambda_{I,I}^0}\right] \right\}, \quad (8)$$

where ξX_I^Φ is the atomic fraction of the solute in layer ξ [13]. As it is difficult to determine I_I^0

accurately, so-called “standardless” methods are applied where I_I^0 is replaced by the intensity of the matrix and appropriate relative sensitivity factors are used to obtain the amount of surface enrichment [11]. To simplify the problem for $\lambda \cong \delta$, it results from Eq. (8) for the first four layers [3,9],

$$\begin{aligned} (I_I/I_I^0)_1 &= 0.63 \times X_I^\Phi, \\ (I_I/I_I^0)_2 &= 0.23 \times X_I^\Phi, \\ (I_I/I_I^0)_3 &= 0.09 \times X_I^\Phi, \\ (I_I/I_I^0)_4 &= 0.03 \times X_I^\Phi. \end{aligned}$$

The sum of these four layers represents 98% of the total intensity, which is a good approximation to 100%. As a consequence, a direct proportionality between X_I^Φ and I_I , $^1X_I^\Phi = (I_I/I_I^0)_1/0.63$ results, if the segregation is confined to the first layer. This approach is generally used to evaluate AES data in studies of segregation (e.g. [7]). For correct determination of the concentration of the atomic layers and the bulk, a calibration of the signal intensity is necessary.

4. Reliability of Quantified AES Data

Sometimes, one can meet in literature a criticism of AES as a technique which is not able to give useful, quantitative data of interfacial segregation (e.g. [14]). It is argued, for example, that “effective value of the quantity $X_I^\Phi/(1-X_I^\Phi)$ which is convolution of the actual plane-by-plane composition” [14] is approximately given by

$$\left(\frac{X_I^\Phi}{1-X_I^\Phi}\right)^{eff} = \frac{\sum_{\xi=1}^N \xi X_I^\Phi \exp[-(\xi-1)\delta/\lambda_{I,I}^0]}{\sum_{\xi=1}^N (1-\xi X_I^\Phi) \exp[-(\xi-1)\delta/\lambda_{I,I}^0]}. \quad (9)$$

Based on Eq. (9) the values of $[X_I^\Phi/(1-X_I^\Phi)]^{eff}$ are calculated in a hypothetical ideal system as being measured in an AES experiment. As a result, its dependence on $1/T$ was obtained similar to that indicated by the dotted line in Fig. 5.

However, the treatment [14] is incorrect. It is based on a wrong solution of the convolution integral in AES [11] by setting the intensity (or “effective quantity”) of each layer equal to the summary concentration of that and all following layers. In other words, in the treatment [14] only the attenuation factor f_w (Eq. (7)) is considered and the correction factor for the concentration of a layer with limited thickness that is detected by AES (Eq. (8)) is ignored. As a consequence, the “effective quantity”, i.e. the sum in the nominator

is getting larger than the homogeneous bulk concentration if ${}^{\xi}X_I^{\Phi} = \text{const} = X_I$ (in contrast to Eq. (8)). This contradiction is the cause of the strange curvature of the dotted line in Fig. 5. In AES, the intensities of Auger electrons are measured and thus $(X_I^{\Phi})^{\text{eff}} = (I_I/I_I^0)_{\text{total}}$. Supposing segregation at the (111) surface confined to one monolayer as calculated in [14] we get for the normalized Auger intensity $(I_I/I_I^0)_1 = 0.63 \times {}^1X_I^{\Phi}$ according to Eq. (8) with $\delta/\lambda = 1$, and the correct Langmuir–McLean segregation isotherm (cf. Eq. (1)) is

$$\ln\left(\frac{{}^1X_I^{\Phi}}{1-{}^1X_I^{\Phi}}\right)^{\text{eff}} = \ln\left\{\frac{\frac{(I_I/I_I^0)_1}{0.63}}{\frac{(I_I^0/I_I^0)_1 - (I_I/I_I^0)_1}{0.63}}\right\} = \ln\left\{\frac{\frac{(I_I/I_I^0)_1}{0.63}}{1 - \frac{(I_I/I_I^0)_1}{0.63}}\right\} \quad (10)$$

$$\ln X_I + \Delta S_I^0 / R - \Delta H_I^0 / RT = a - bT.$$

It is obvious that the linearity with $1/T$ is attained by setting the maximum possible Auger intensity for a complete monolayer, $X_I^{\Phi} = 1$, to $(I_I/I_I^0)_1 = 0.63$ (i.e. correct calibration for the AES intensity with respect to $X_I^{\text{bulk}} = 1$). A completely linear dependence of $\ln[{}^1X_I^{\Phi}/(1-{}^1X_I^{\Phi})]$ on $1/T$ follows from Eq. (10), (Fig. 5). In contrast, Eq. (9) adds up to a value 1.59 of 100% bulk intensity for $\delta/\lambda = 1$. Therefore, the “effective” concentrations are ${}^1X_I^{\Phi,\text{eff}} = (I_I/I_I^0)_1/1.59$ while $X_I^{\Phi} = (I_I/I_I^0)_1 = 1$. This is equivalent to $\ln[{}^1X_I^{\Phi}/(1.59-{}^1X_I^{\Phi})]$ for the left hand side of Eq. (10). As a consequence, the dotted line in Fig. 5 is obtained. The remark about the “asymptotic” behavior of the line is by no means coming “...from the persistence of AES signal from the substrate...” [14] but from a wrong approach to quantitative evaluation of the AES intensities [9].

AES measurements of interfacial segregation are also sometimes misinterpreted by taking the ratio of the measured peak intensity of the solute to that of the matrix, (I_I/I_M) , as proportional to X_I^{Φ} . It is mainly because it is difficult to perform measurements under the same experimental conditions and therefore, the matrix intensity, measured at the same time as the solute signal, is taken as “internal standard”. This ratio technique

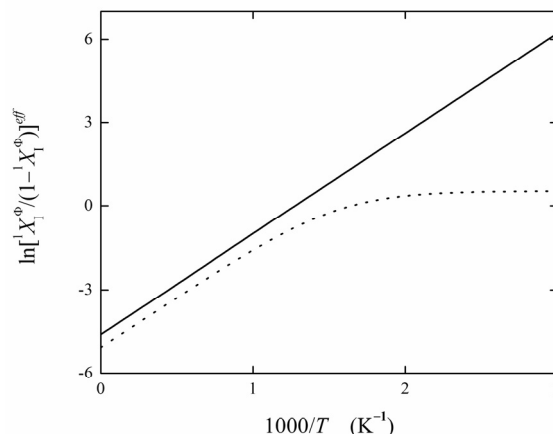


Fig. 5. Quantification of AES data of surface segregation. Plot $\ln[{}^1X_I^{\Phi}/(1-{}^1X_I^{\Phi})]^{\text{eff}}$ vs. $1/T$ which is expected in an AES experiment for a (111) surface in an ideal system with $\Delta S_I^0 = 0$ and $\Delta H_I^0 = -30$ kJ/mol. Correct (full line) and incorrect (dotted line) quantification for monolayer segregation is shown [3].

is very useful, however, its interpretation has to be done correctly (e.g. [3,8]). A serious problem with application of the data on grain boundary segregation may also occur when the AES results are incorrectly treated. This is frequently done when the data are averaged (i) over the total segregation depth; (ii) for differently concentrated $M-I$ alloys; and (iii) for various interfaces/sites (i.e. neglecting the anisotropy of interfacial segregation) [3]. Probably the latter case is the most frequent one because grain boundary segregation is usually measured at various non-specified boundary facets of a polycrystalline material and thus, these data do not characterize any single interface. Moreover, AES data measured in different samples (for example, annealed at various temperatures) reflect the behavior of different grain boundaries. Such data should be neither compared nor used to determine thermodynamic characteristics of grain boundary segregation (enthalpy and entropy) because such values are “effective” without physical meaning [3,15]. Similarly, temperature dependence of average grain boundary concentrations measured in differently concentrated $M-I$ alloys (item (ii)) provides us with effective values of segregation enthalpy and entropy (e.g. [16]). It is strange if such data are used for generalization and mainly to dishonest AES (e.g. [14,17]) although correctly interpreted data well agree with all dependences and predictions [18]. Another misunderstanding arises from misinterpretation of physically meaningless effective variables for well defined

standard enthalpy and entropy of grain boundary segregation [14]. The main reason for it is an apparent similarity of these two sets of parameters – both standard and effective counterparts (enthalpy and entropy) are independent of temperature and concentration [19]. Despite this apparent similarity the effective and standard segregation enthalpy and entropy are completely different as is clearly seen from Fig. 6.

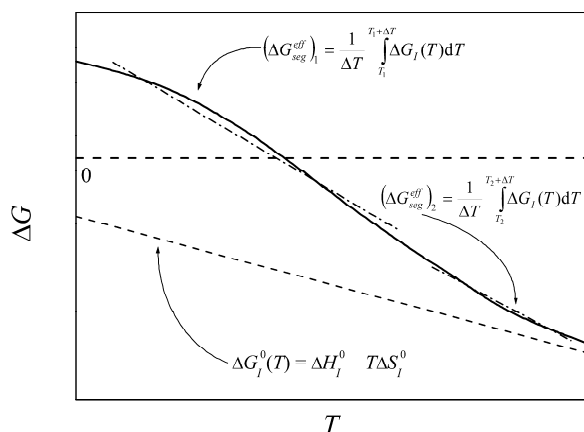


Fig. 6. Schematic comparison of the standard Gibbs energy of segregation and effective Gibbs energy of segregation showing apparently similar behavior (i.e. apparently constant ΔH_{seg}^{eff} and ΔS_{seg}^{eff}) but obviously their different values [19].

5. Conclusions

The specifics of quantification of AES spectra to composition of grain boundaries are discussed. It is shown that incorrect quantification results in misleading values of the concentration and consequently, physically meaningless values of the thermodynamic parameters of segregation. If the quantification is performed in a correct way, AES remains one of the best methods to determine grain boundary segregation at monolayer scale and provides us with the data which can be used in generalized form for many applications.

Acknowledgement

Financial support of the CSF (106/08/0369) is gratefully acknowledged.

References

- [1] E.D. Hondros, M.P. Seah, S. Hofmann and P. Lejček, in *Physical Metallurgy*, 4th Edn., ed. by R.W. Cahn and P. Haasen, pp. 1201–1289, North-Holland, Amsterdam (1996).
- [2] D. McLean, *Grain Boundaries in Metals*, Clarendon, Oxford (1957).
- [3] P. Lejček and S. Hofmann, *Crit. Rev. Sol. State Mater. Sci.* **33**, 133 (2008).
- [4] P. Lejček and S. Hofmann, *Surface Sci.* **307–309**, 798 (1994).
- [5] S. Suzuki, K. Abiko and H. Kimura, *Scripta Metall.* **15**, 1139 (1981).
- [6] P. Lejček and S. Hofmann, *Crit. Rev. Sol. State Mater. Sci.* **20**, 1 (1995).
- [7] M. Menyhard, B. Rothman, C.J. McMahon, Jr., P. Lejček and V. Paidar, *Acta Metall. Mater.* **39**, 1289 (1991).
- [8] P. Lejček, *Anal. Chim. Acta* **297**, 165 (1994).
- [9] S. Hofmann and P. Lejček, *Int. J. Mater. Res.* **100**, 1167 (2009).
- [10] C.J. Powell and A. Jablonski, *NIST Electron Effective-Absorption-Length Database, Version 1.0 (SRD 82)*, US Dept. of Comm., NIST, Gaithersburg (2001).
- [11] S. Hofmann, in *Practical Surface Analysis*, 2nd Edn., Vol. 2, ed. by D. Briggs and M.P. Seah, pp. 156–161, Wiley, Chichester (1990).
- [12] K.D. Childs, B.A. Carlson, L.A. LaVanier, J.F. Moulder, D.F. Paul, W.F. Stickle and D.G. Watson, *Handbook of Auger Electron Spectroscopy*, 3rd Edn., Physical Electronics, Eden Prairie (1995).
- [13] M.P. Seah, in *Practical Surface Analysis*, 2nd Edn., Vol. 1, ed. by D. Briggs and M.P. Seah, pp. 201–255, Wiley, Chichester (1990).
- [14] P. Wynblatt and D. Chatain, *Metall. Mater. Trans. A* **37**, 2595 (2006).
- [15] P. Lejček, *Mater. Sci. Eng. A* **185**, 109 (1994).
- [16] R. Mast, H. Viehhaus and H.J. Grabke, *Steel Res.* **70**, 239 (1999).
- [17] C.L. Briant, *Phil. Mag. Lett.* **73**, 345 (1996).
- [18] P. Lejček, *J. Alloy Compd.* **378**, 85 (2004).
- [19] P. Lejček, *Grain Boundary Segregation in Metals*, Springer (2010).